Comparison between asymmetric and symmetric stereoscopic DPIV system

by

S. Coudert[*], J. Westerweel[**] and T. Fournel[*]

[**] Laboratory for Aero and Hydrodynamics
Delft University of Technology
Rotterdamseweg 145, 2628 AL Delft, The Netherlands

[*] Laboratory of "Traitement du Signal et Instrumentation" - UMR CNRS 5516
J. Monnet University
23 rue du Docteur Paul Michelon, 42023 Saint-Etienne CEDEX 2, France

ABSTRACT

Measuring the 3 components of the velocity in a large area of a turbulent flow requires the stereoscopic DPIV system. On most flow facilities, positioning the camera in a symmetric way is not possible. The accuracy may change between different angle set-up.

Asymmetric and symmetric set-up are compared using an angular stereoscopic DPIV system with Scheimpflug conditions. The data consist of nine set-up with different camera angles. The measured displacement is compared to the actual displacement of a paper pattern mounted on a 3D translation stage. The warping method followed by a geometrical reconstruction are used to compute 3D vector field.

The main accuracy behaviours of the angle set-up are depicted using mainly the aperture angle aa (angle in between the two camera) and asymmetry angle (difference of camera angles).

Simple rules can be laid out such as:

- the more asymmetric is the set-up and the larger is the aperture angle, the more accurate the system is
- high aperture angle should be preferred to the location of the stereoscopic system
- symmetric system with a aa around 60° is a good compromise, regarding to accuracy and space consuming

Table 2 : all angle configurations tested

angle of camera		angle between camera	
left (la)	right (ra)	aperture (aa)	asymmetry (sa)
+15°	+15°	+30°	+00°
+30°	+00°	+30°	+30°
+30°	+15°	+45°	+15°
+30°	+30°	+60°	+00°
+45°	-15°	+30°	+60°
+45°	+00°	+45°	+45°
+45°	+15°	+60°	+30°
+45°	+30°	+75°	+15°
+45°	+45°	+90°	+00°

the left and the right camera angle are named respectively la and ra; the aperture angle aa (aa=la+ra) is the angle between the camera; the asymmetry angle sa (sa=la-ra), is the difference between the left and right angle regarding the central position +00°, it is ment to represent the asymmetry of the configuration.

INTRODUCTION

Measuring the 3 components of the velocity in turbulent flow requires the stereoscopic DPIV system, for large viewing area. The two cameras are positioned regarding to the laser sheet with two different angles of view. In order to collect the maximum light from the laser sheet, the lens systems of the cameras need to be wildly open. So the focal depth is very narrow. In this conditions, two main system are used: the so-called translation displacement system and the angular one. On most flow facilities, positioning the cameras in a symmetric way is not possible. The accuracy may change between configurations with different angles.

The stereoscopic set-up and the processing steps that we used were designed by J.van Oord (1997). The main advantage of the 2D3C angular stereoscopic DPIV technique used with Scheimpflug conditions is that it permits to collect the maximum light from the light sheet. This technique is also easy to set-up and to use compared to complex mechanical system such as in Lawson and Wu (exp.1997) and Soloff et al (1997). This system is preferred to the translation one since a viewing angle can be used up to around 45°. A viewing angle of 45° is theoretically the most accurate angle referring to Lawson and Wu (th.1997). Using angular and Scheimpflug conditions introduce distortions on the recorded images. Also second order "connecting functions" are used to connect the CCD-chip plane to the object plane. The warping technique is preferred to the mapping one, as it have the same accuracy and is less computational time consuming (e.g. Coudert and Westerweel (2000)).

Different angle configurations are tested: symmetric and asymmetric set-up for different values of the angle between the cameras. As in literature differences are found between theory and experiment (e.g. Lawson and Wu (exp.1997)), the accuracy of the different configurations is tested on a test pattern mounted on a 3 dimensional translation stage, by comparing the actual displacement and the measured one.

SET-UP

The 2D3C stereoscopic DPIV set-up is composed of 2 Texas-Instrument High-Resolution CCD cameras (1000x1016 pixel) and 2 Nikon 55 mm macro lenses mounted on a flat ring. The lenses are separated from the camera in order to shift the CCD-chip plane regarding to the lens plane so the Scheimpflug conditions are satisfied. For more information on the mechanical tilt system refers to Oord (1997).

A sticky and flat plate is mounted on a 3D translation stage in the viewing area of the 2 cameras. Different printed paper patterns can lay on this sticky plate. Two types of patterns are used: pattern of dots on a regular grid (also called dot pattern) and pattern of random coordinates points (DPIV pattern). Warping coefficients are computed help to a dot pattern and displacements onto recorded images of a DPIV pattern. As the 3D displacements realised are uniform, statistics of the fields of 3D vector can be computed. The accuracy of the translation stage is 5 µm.

Using the flat ring, the distance between both optics and the sticky plate is constant for every angle and has a value of 210 mm. Holes in this flat ring permit to mount cameras with angles in the range between 0° and 45° with steps of 15° regarding to the normal position of the sticky plate plane (c.f. Figure 1). The minimum angle between the two cameras is 30° as the camera it self and the lenses are space consuming.

PROCESSING

The recorded DPIV images are processed using a standard DPIV cross-correlation algorithm to assess the 2D vectors. Then, the 2D vectors are back-projected in the object plane using a warping method. The two previous steps are run for both cameras. Finally, a geometric reconstruction of the 3D vectors DPIV is done using the 2D warped vectors and the set-up geometry. These three steps are fully described in the next paragraphs.

The recorded DPIV images are processed by a standard cross-correlation algorithm using FFT on 32 pixel width interrogation window with a 50 % overlap. The algorithm is in two pass: a first field of vector is computed then its vectors are smoothed on its neighbours; the second pass consists of processing the DPIV images with a window shifting using the previous smoothed vector field (e.g. Westerweel et al (1997)).

The back-projection in the object plane of the 2D vectors computed in the previous step, is done using the second order polynomial warping method. This warping method consists to connect the CCD-chip plane to the object plane with "connecting functions". The "connecting functions" used are second order polynomials in order to take in account the distortions due to the viewing angle and the optical distortions induced by the lenses. The coefficients of the "connecting functions" are determined using the co-ordinates of dot centres. These dots come from a pair of images recorded on a dot pattern. This dot pattern determines the object plane. Every vector is back-projected from the image field to the object field using the warping "connecting functions". The vectors of the two object fields of left camera and right camera are neighbourhood interpolated on a common rectangular grid in the object plane (e.g. Oord (1997)).

Finally, the 3D vectors of the displacement are reconstructed from the previous warped 2D vectors, using the set-up geometry. The reconstruction equations for symmetric set-up can be found in Oord (1997). For asymmetric

set-up, the components (U,V,W), along (X,Y,Z) axis, of a 3D displacement lay in Figure 2 and are depicted in Table 1.

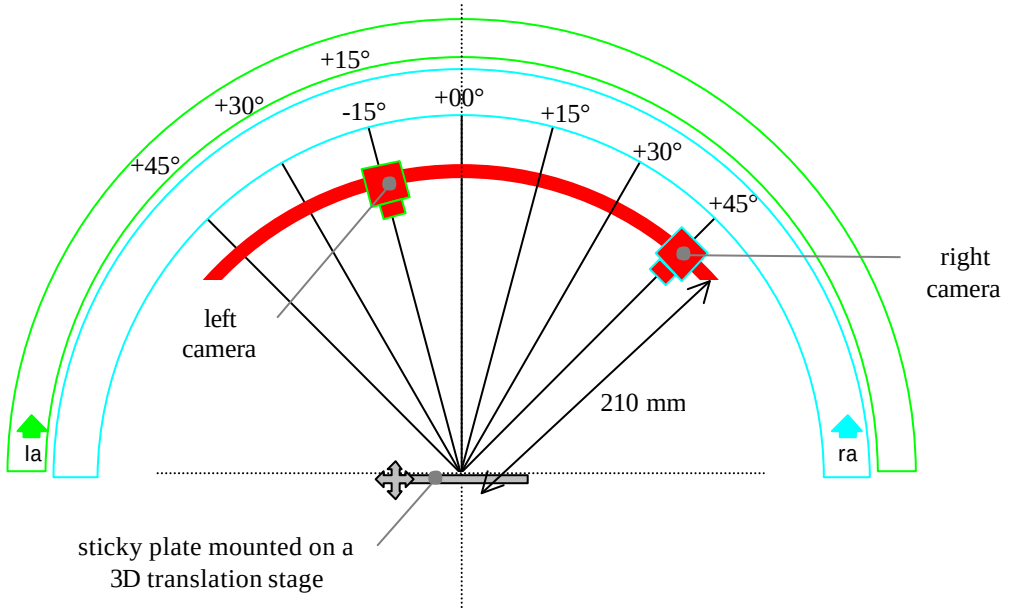

Figure 1 : angular SDPIV set-up.

Table 1 : reconstruction equations for asymmetric set-up

components		with
$W = \frac{U_l - U_r}{T_{.l} + T_{.r}}$		$T_{.l} = \frac{B_{0l} + (X_0 + U_l)}{H_{0l}}$
$U = \frac{(-W \times T_l + U_l) + (W \times T_r + U_r)}{2}$	is a mean value	$T_{.r} = \frac{B_{0r} - (X_0 + U_r)}{H_{0r}}$
$V = \frac{V_{.l} + V_{.r}}{2}$	is a mean value	$V_{.i} = -W \frac{V_i + Y_0}{H_{0i}} + V_i$
		$B_{0i} = d_{0i} \sin q_i$
		$H_{0i} = d_{0i} \cos q_i$
		i = l or r

l and r indices represent left and right. d_0 and θ represent respectively the distance between the center of the lens and the object plane and the viewing angle of the camera regarding to the normal to the object plane.
U, V and W are the components of the 3D displacement vector respectively along X, Y and Z axis. (U_l, V_l) and (U_r, V_r) are the components of the 2D warped vector respectively for left and right cameras. As two equations can be computed to calculate the V component, the mean value of $V_{.l}$ and $V_{.r}$ is taken as the value of V, idem for the U component.

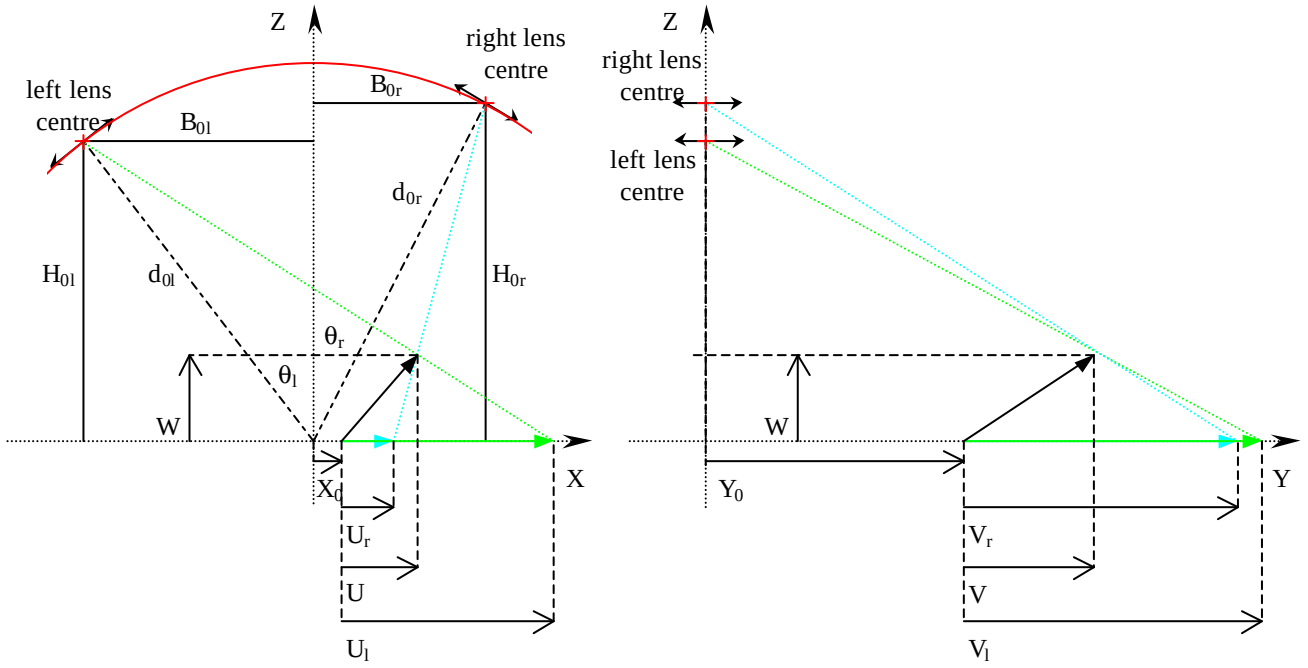

Figure 1 : ray tracing for geometric reconstruction.

EXPERIMENTS

Nine different angle configurations are realised using the set-up described in the previous paragraph. The angles for the left and right camera (respectively la and ra) and the corresponding aperture angle aa and asymmetry angle sa lay in table 2. The aperture angle, computed as (la+ra), describes the angle between the two cameras, whereas the asymmetry angle , computed as (la-ra), depicts the asymmetry of the set-up regarding to the normal of the object plane (angle=+00°).

Table 2 : all angle configurations tested

angle of camera		angle between camera	
left (la)	right (ra)	aperture (aa)	asymmetry (sa)
+15°	+15°	+30°	+00°
+30°	+00°	+30°	+30°
+30°	+15°	+45°	+15°
+30°	+30°	+60°	+00°
+45°	-15°	+30°	+60°
+45°	+00°	+45°	+45°
+45°	+15°	+60°	+30°
+45°	+30°	+75°	+15°
+45°	+45°	+90°	+00°

the left and the right camera angle are named respectively la and ra; the aperture angle aa (aa=la+ra) is the angle between the camera; the asymmetry angle sa (sa=la-ra), is the difference between the left and right angle regarding the central position +00°, it is ment to represent the asymmetry of the configuration.

For each angle set-up, the experiment run in 2 steps.
Firstly, the connections between the object plane and the CCD-chips of both camera are realised by recording a pair of images from a pattern of dots on a regular grid. At this step, the Scheimpflug angle of the CCD-chip is adjusted help to live displaying the images of each camera. The Scheimpflug angle adjustment can be accurately reached with the lowest number of aperture of the lens, as the depth of focalisation is the narrowest. Using Nikon 55 mm macro lenses with a 2.8 number of aperture, the Scheimpflug angle can be reached with more or less a precision of 1°.

Secondly, DPIV images are recorded from a DPIV paper pattern (random points all over the paper). This pattern is mounted on a 3D-translation stage with a positioning accuracy of 5 µm. A pair of images for (X,Y,Z)=(0,0,0) position is recorded and also for different displacements along the axes using the 3D translation plate. The displacements tested range from 0 µm to 600 µm by steps of 200 µm along X and Z axis. The displacements of the DPIV pattern are uniform displacements along the 3 axes.
Then, coefficients of the "connecting functions" for the warping method are computed for both camera on the pair of dot images recorded in the first step. And the recorded DPIV images are processed using the pipeline described in the PROCESSING paragraph to reach a field of 3D vectors for each displacement. Finally statistics of the whole fields are computed as 3D actual displacements are uniform.

RESULTS AND DISCUSSION

A sum-up of all the notations used in this paper can be found at the end of the document.
The statistics of the measured 3D vector fields are compared against the actual displacement.
As the accuracy of the 3D translation stage is about the same as the measurement one, the data is fluctuating regarding to absolute variables such as the bias error and consequently on the bias error ratio. But, as described in the following the bias error ratio seems to follow also the same behaviour comparing symmetric to asymmetric set-up.
For all the data, the rmsX, which corresponds to the rms value for a displacement along the X axis, is quite constant and around 10 µm. Whereas for rmsZ, it value fluctuate from the best accuracy, reached for symmetric set-up with an aperture angle aa>=60°, around 10 µm to the worst accuracy, reached for an asymmetric set-up with la=+45° and ra=-15°, around 25 µm. Also, the error ratio er, found in Lawson and Wu (th.1997), computed as the rms value for dZ divided by the rms value for dX for the same displacement d (d=dX=dZ), depict the differences of accuracy between the different set-up. Indeed, the bias error ratio ber, computed in the same way as the ratio of the bias errors beX and beZ respectively for dX and dZ displacements, have the same behaviour as er. The total error is an accumulation of both error ratio but the main behaviours are depicted by one of them.
Only the displacement by the amount of 400 µm is plotted in this paragraph. For symmetric set-up, the theoretical error ratio and the experimental error ratio er, used in Lawson and Wu (th.1997), is plotted in Figure 3. The experimental error ratio behaves according to the theoretical error ratio, also named as random error ratio, and these results are comparable to the results found by Lawson and Wu (exp.1997).

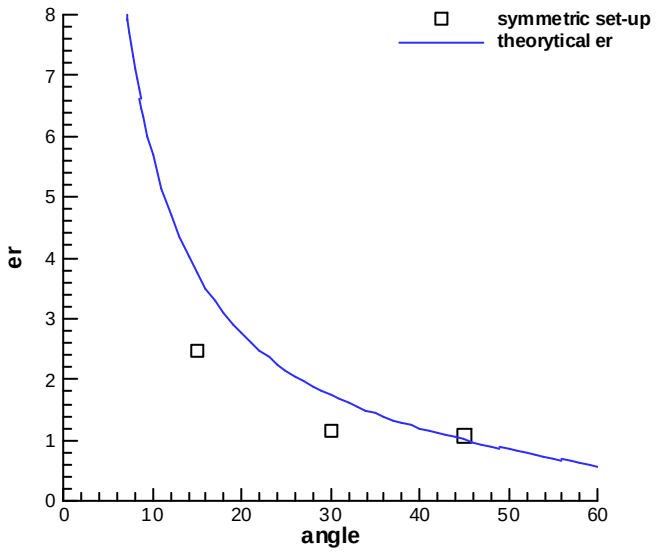

Figure 2 : error ratio er is plotted against the angle for symmetric set-up; displacement is dX=dZ=400 µm; the angle is equal to the left and the right camera angle; the theoretical error ratio found in Lawson and Wu (th.1997) is plotted in continuous line (er=1/tan(angle)).

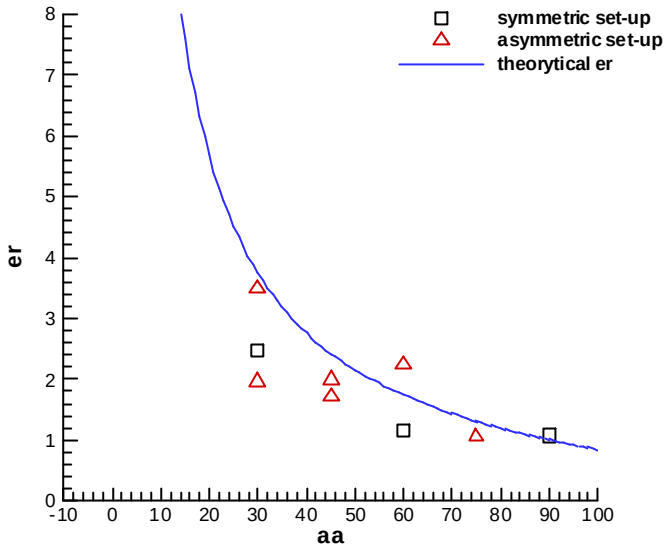

Figure 3 : the error ratio er is plotted against the aperture angle aa (aa=la+ra); square points represent symmetric stereoscopic set-up and triangle points asymmetric stereoscopic set-up ; the theoretical er for symmetric set-up is plotted in continuous line (er=1/tan(aa/2)).

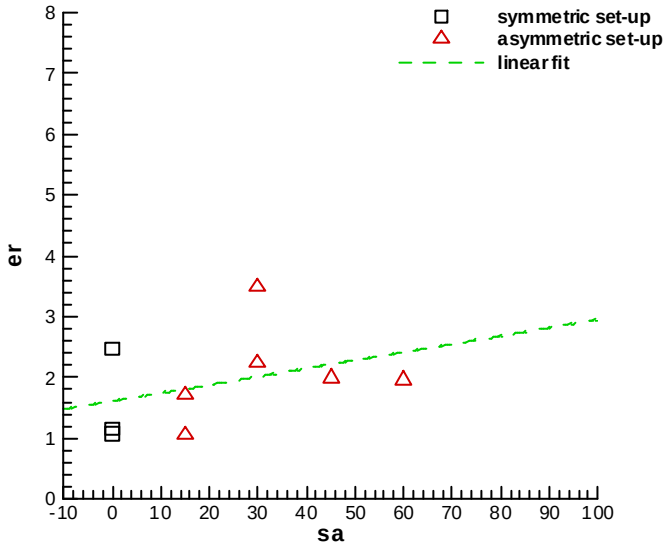

Figure 4 : the error ratio er is plotted against the aperture angle sa (sa=la-ra); square points represent symmetric stereoscopic set-up and triangle points asymmetric stereoscopic set-up ; the linear fit for all data is plotted in dashed line.

Considering all the data, the bias error be between actual displacement d and measured displacement m is rising, for displacement along the Z axis, regarding to the generated displacement d. But the bias error ratio ber, between the absolute value of the displacement error be and the generated displacement d is 2% ± 2% of the in-plane displacements dX, and 9% ± 4% of the out-of-plane displacements dZ. Whereas, the rms value stays between 0.5% and 1.5% of dX and 1% and 4.5% of dZ. These values are fluctuating regarding to the angles and the actual displacement; such behaviour is also found in Lawson and Wu (exp.1997).
For the configuration with the left camera at +45°, the bias error ratio ber for the X displacement is less than 4% regarding to the different angles of the other camera, whereas for the Z displacement, ber seems increase following a slope of 1% per 10°; also, changing the angle of the right camera by an amount of -10°, increases the

error of the out-of-plane component by 1%, if the left camera is at +45°. The experimental error ratio er is plotted for the same left camera angle (la=+45°) against the ra. The er value is fluctuating regarding to the ra; but reasonably it could be said that the ra have no effect on the er. Consequently, the effect of changing the right angle with the same left angle have no effect on the consistence of the DPIV cross-correlation processing, even if there is a difference of magnification on the images processed, and of course even if the common zone, where both camera areas overlap, is smaller.

For all set-up and a 400 µm displacements, the error ratio er is plotted in figure 4 as a function of the aperture angle aa which is the sum of the left angle and the right angle. So, configurations with the same aa between both cameras can be compared at the same abscissa. Furthermore, the accuracy of the configurations with respect to the aperture angle aa between both cameras can be compared. The er decreases as the aperture angle aa increases; this is confirmed by the theory: the accuracy on the out-plane component increases with the aperture angle aa between the two cameras increases.

In order to get an idea of the difference between symmetric and asymmetric configurations, the data is plotted subtracting the left angle to the right angle (figure 5). In this figure, symmetric configurations are at abscissa 0 and the bigger abscissa value is concerned, the more asymmetric is the system. The er increases regarding to the asymmetry angle sa increases. In other words, the accuracy on the out-of-plane component decreases while the configuration get more asymmetry.

CONCLUSION

An angular SDPIV system with Scheimpflug conditions is tested on a mechanical test bench. This bench permit to compare actual displacement of a DPIV test pattern to the measured displacement. As the displacement made is uniform, statistics of the measured 3D vector field permit the computation of the accuracy of a measurement set-up. The accuracy behaviour of nine angle set-up is depicted. Simple rules can be laid such as: the more asymmetric is the set-up and the larger is the aperture angle, the more accurate the system is.

To conclude, high aperture angle should be preferred to perpendicular location of the whole stereoscopic system to the objet plane (asymmetry). And symmetric system with a aa around 60° is a good compromise, regarding to accuracy and space consuming.

FUTURE

As accuracy of the 3D translation stage is around the accuracy of measurement system, the mean value of the measured displacement is not much stable, more data needs to be acquired with a higher accuracy of the displacement system. Also, the set-up needs to be automated at least for the displacement of the test pattern.

Tests on a test pattern are of course different from measuring in an actual flow illuminated by a laser light sheet. In order to test the accuracy of this stereoscopic method, a transparent resin block with particles in it, should be used instead of the paper pattern: it does represent much more reality, especially for particles moving in and out of the laser sheet.

Measurement of turbulence in a pipe flow is under investigation. The error induced by the misalignment of the laser sheet and the object plane is not shown in this paper. Using a correction approach on a special vector field, more accurate result should be found. This correction approach is based on a mapping algorithm. This mapping algorithm is used in Willert (1997) and compared to warping algorithm in Coudert and Westerweel (2000). In addition, an automatic calculation of the angles and the positions of the cameras is under investigation.

REFERENCES

Coudert, S. and Westerweel, J. (2000). "Comparison between warping and mapping methods on a Stereoscopic 2D3C DPIV system with Scheimpflug", EuroMech 411, Rouen, France, 29-30 May 2000.

Lawson, N. and Wu, J. (th.1997). "Three-dimensional particle image velocimetry: error analysis of stereoscopic techniques", Measurement science and technology, 8, pp. 894-900.

Lawson, N. and Wu, J. (exp.1997). "Three-dimensional particle image velocimetry: experimental error analysis of digital angular stereoscopic system", Measurement science and technology, 8, pp. 1455-1464.

Oord, J. van (1997). "The design of a stereoscopic DPIV system", MEAH Report 161, Delft University of Technology. (Also available as EuroPIV Report 07PT14.)

Soloff, S., Adrian, R. and Liu, Z.-C. (1997), "Distortion compensation for generalised stereoscopic particle image velocimetry", Measurement science and technology, 8, pp. 1441-1454

Westerweel, J., Dabiri, D. and Gharib, M. (1997), "The effect of a discrete window offset on the accuracy of cross-correlation analysis of a digital PIV recordings", Experiment in fluids, 23, pp. 20-28.

Willert, C. (1997), "Stereoscopic digital particle image velocimetry for application in wind tunnel flows", Measurement science and technology, 8, pp. 1465-1479

NOTATIONS

la	left camera angle
ra	right camera angle both la and ra angles are the angles between the plane perpendicular to the pattern and the optical axis of the lens of the respective camera
aa	aperture angle, aa is the angle between the 2 camera computed as (la+ra)
sa	asymmetry angle computed as (la-ra) with (la>=ra)
d	displacement generated with the translation plates dX and dZ are respectively d along X and Z axes
m	mean value of $m_{i,j}$ on a 3D vector field for a single d mX and mZ are respectively m for dX and dZ
be	bias error between d and m, computed as (d-m) beX and beZ are respectively be for dX and dZ
ber	bias error ratio, computed as (beZ/beX)
rms	rms value of $m_{i,j}$ on a 3D vector field for a single d rmsX and rmsZ are respectively rms for dX and dZ
rmsr	rms ratio between the rms and d, computed as (rms/d) rmsrX and rmsrZ are respectively rmsr for dX and dZ
er	experimental error ratio, computed as (rmsZ/rmsX)